Tensile-Strain-Dependent Spin States in Epitaxial $LaCoO_3$ Thin Films

Y. Yokoyama,[1,2,*] Y. Yamasaki,[3,4,5] M. Taguchi,[6,†] Y. Hirata,[1,2] K. Takubo,[1] J. Miyawaki,[1] Y. Harada,[1] D. Asakura,[7] J. Fujioka,[3] M. Nakamura,[4] H. Daimon,[6] M. Kawasaki,[3,4] Y. Tokura,[3,4] and H. Wadati[1,2]

[1]*Institute for Solid State Physics, University of Tokyo, Chiba 277-8581, Japan*
[2]*Department of Physics, University of Tokyo, Tokyo 113-0033, Japan*
[3]*Department of Applied Physics and Quantum-Phase Electronics Center (QPEC), University of Tokyo, Hongo, Tokyo 113-8656, Japan*
[4]*RIKEN Center for Emergent Matter Science (CEMS), Wako 351-0198, Japan*
[5]*National Institute for Materials Science (NIMS), Tsukuba 305-0047, Japan*
[6]*Nara Institute of Science and Technology (NAIST), 8916-5, Takayama, Ikoma, Nara 630-0192, Japan*
[7]*Research Institute for Energy Conservation, National Institute of Advance Industrial Science and Technology (AIST), Umezono 1-1-1, Tsukuba 305-8568, Japan*

(Received 24 August 2017; published 17 May 2018)

The spin states of Co^{3+} ions in perovskite-type $LaCoO_3$, governed by the complex interplay between the electron-lattice interactions and the strong electron correlations, still remain controversial due to the lack of experimental techniques which can directly detect them. In this Letter, we revealed the tensile-strain dependence of spin states, i.e., the ratio of the high- and low-spin states, in epitaxial thin films and a bulk crystal of $LaCoO_3$ via resonant inelastic soft x-ray scattering. A tensile strain as small as 1.0% was found to realize different spin states from that in the bulk.

DOI: 10.1103/PhysRevLett.120.206402

Charge, spin, and orbital degrees of freedom activated by a strong electron correlation realize emergent physical phenomena such as superconductivity, metal-insulator transition, and charge ordering [1]. The perovskite-type cobalt oxide $LaCoO_3$ is one of the most intriguing materials due to its versatile electron degrees of freedom. Since the spin state of $LaCoO_3$ is sensitive to the crystal field, it shows a spin crossover from the low-spin (LS) to high-spin (HS) state with increasing temperature [2]. In addition, the spin states can be modified by external stimuli such as a magnetic field and pressure. For example, the possibility of an excitonic insulating state under a high magnetic field was theoretically proposed in the bulk crystal and has also attracted considerable interest these days [3–5]. Epitaxial strain can also influence the spin states as observed for ferromagnetism in $LaCoO_3$ thin films at lower temperatures ($\lesssim$85 K) [6–13].

The crystal structure of bulk $LaCoO_3$ is a rhombohedral perovskite-type with corner-sharing CoO_6 octahedra, in which the valence of Co is 3+ with a $3d^6$ configuration. The spin state of $LaCoO_3$ is considered to take a LS state with $e_g^0 t_{2g}^6$, intermediate-spin (IS) state with $e_g^1 t_{2g}^5$, or HS state with $e_g^2 t_{2g}^4$. The population of HS state gradually increases as the temperature increases from around 100 K and the HS state becomes dominant above 500 K [2]. Although the spin state and its temperature dependence of $LaCoO_3$ bulk have already been studied by using various experimental and theoretical approaches [14–21], the spin states have not been completely determined yet. Especially, the spin states in the intermediate temperature region remain controversial, i.e., the mixed HS/LS state or the IS state. On the other hand, in ferromagnetic $LaCoO_3$ thin films, it is indicated that the ferromagnetism originates from the spin state, orbital, and spin orderings [11–13]. From the resonant x-ray diffraction, modulation vector $\boldsymbol{q} = (1/4, -1/4, 1/4)_{\mathrm{pc}}$ (the suffix pc stands for the pseudocubic setting) and $\boldsymbol{q} = (1/6, 1/6, 1/6)_{\mathrm{pc}}$ were observed in the thin films grown on LSAT(110) and LSAT(111) substrates, respectively [LSAT: $(LaAlO_3)_{0.3}(SrAl_{0.5}Ta_{0.5}O_3)_{0.7}$]. Then, the spin states are considered to depend on the tensile strain. In these thin films, some possible models of spin state orderings were reported in Refs. [11,12]. The proposed relationships between the strain and the estimated ratio of spin states per unit cell are shown in Table I. The change of lattice constant and symmetry induced by the tensile strain are the main factors that determine the spin state.

In previous studies, the spin states were conjectured from the orderings of $3d$ electrons on the basis of resonant x-ray diffraction [11–13]. However, direct observations of the electronic structures are needed to clarify the spin states.

TABLE I. The estimated ratio of spin states per unit cell at the lowest temperature in the previous studies [2,11,12]. A positive value of strain indicates a tensile strain.

	Strain (%)	LS :	IS :	HS
$LaCoO_3$ bulk [2]	0	1	0	0
$LaCoO_3$/LSAT(111) [12]	0.5	2	0	1
$LaCoO_3$/LSAT(110) [11]	1.0	0	3	1

Since it is difficult to determine the HS/LS ratio by conventional methods such as x-ray absorption spectroscopy (XAS), we performed resonant inelastic soft x-ray scattering (RIXS) by using Co $2p \rightarrow 3d \rightarrow 2p$ process (L edge). The RIXS is one of the most powerful techniques to clarify the spin states by observing the d-d excitations [22–24]. A higher-energy resolution (a few hundreds of meV) is required to distinguish the d-d excitations from the elastic scattering [16].

The $LaCoO_3$ epitaxial thin films with the thickness of 30 nm were fabricated on LSAT(110) and LSAT(111) substrates by pulsed laser deposition technique. By using the same substrates with different orientations, we can obtain the pure strain effects on XAS and RIXS spectra. In addition, the LSAT substrate has no structural phase transition and thus suitable for the temperature dependent measurements. Details for the syntheses and the characterizations were described in Refs. [11,12]. The lattice constant of the LSAT substrate is 3.868 Å, while that of the $LaCoO_3$ bulk is 3.804 Å [25], meaning that the $LaCoO_3$ epitaxial thin films grown on LSAT substrates are distorted by tensile strain. The tensile strains from LSAT(110) and LSAT(111) substrates are 1.0% and 0.5%, respectively (strains are defined as the ratio of the cubic root of the unit cell volume) [11,12]. The experiments of XAS and RIXS were performed at BL07LSU HORNET, SPring-8 [26]. Before RIXS measurements, we obtained the XAS spectra at 300 K by total electron yield (TEY) in order to determine the excitation energy of RIXS. The RIXS measurements were performed at 40 and 300 K by using soft x-ray from 770 to 810 eV (Co $L_{3,2}$ edge). In the range of the x-ray energy, energy resolution $\Delta E \sim 300$ meV, which was determined via full width at half maximum (FWHM) of the elastic peak. The charge coupled device (CCD) detector was set at 90° relative to the incident x ray with horizontal polarization to suppress the elastic scattering [see inset in Fig. 1(b)].

First, we measured Co $L_{3,2}$ XAS by TEY mode of $LaCoO_3$ thin films at 300 K. The spectra are shown in Fig. 1(a). The peaks around 779 and 794 eV correspond to the Co L_3 and L_2 edges, respectively. Although the magnitude of the tensile strain and modulation vector q are different between LSAT(110) and LSAT(111), the spectral shapes are quite similar. To investigate the detailed electronic structures from d-d excitations, we performed RIXS measurements. As the excitation energy of RIXS, we selected the energy of A: $L_3 - 2.9$ eV, B: $L_3 - 1.5$ eV, C: $L_3 - 1.0$ eV, D: L_3, E: $L_3 + 1.7$ eV, and F: L_2. The Co $L_{3,2}$ RIXS spectra of the $LaCoO_3$ thin films are shown in Fig. 1(b). These spectra are normalized by the intensity of the highest peak. In this figure, the thick solid line shows the center of the elastic scattering peaks and the arrows indicate the fluorescence ones. Other peaks from 0 to 4 eV correspond to the d-d excitations and the peak around 5.0 eV may be a charge-transfer (CT) excitation. In the

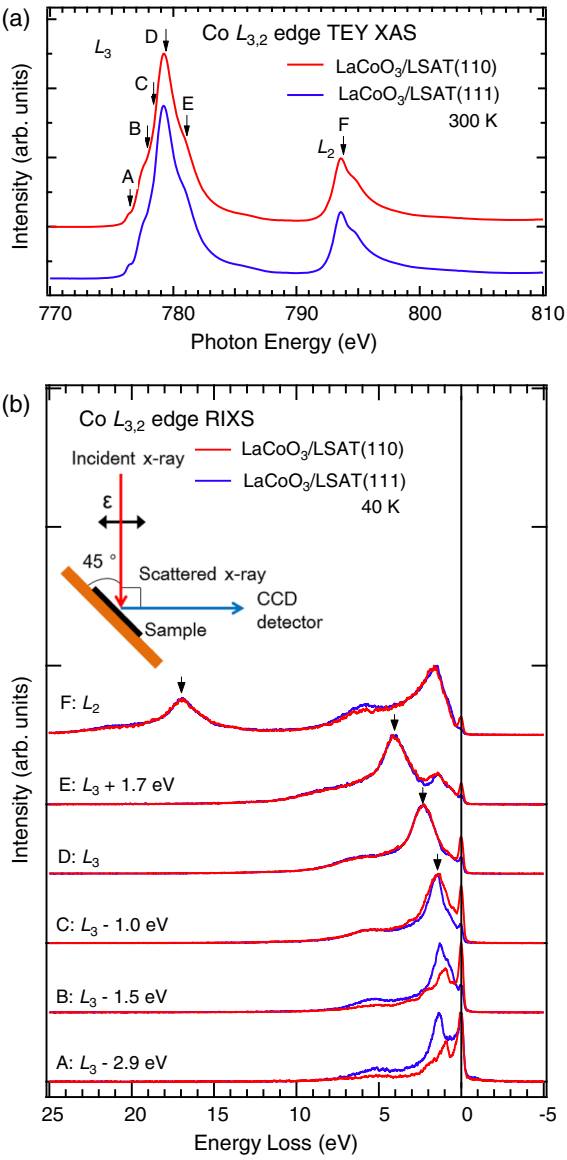

FIG. 1. Spectra measured at the Co $L_{3,2}$ edge by the (a) TEY-XAS and (b) RIXS spectra of $LaCoO_3$ thin films grown on LSAT (110) and LSAT(111) substrates. The arrows and letters in XAS indicate the excitation energies for RIXS. All RIXS spectra are normalized by the intensity of the highest peak and the arrows indicate the fluorescence peaks. The inset shows the schematic diagram of the experimental setup in our RIXS measurements.

spectra of A and B, the peaks of d-d excitations are clearly observed. We find that the d-d excitations are obviously different between the thin films on LSAT(110) with 1.0% tensile strain and LSAT(111) with 0.5% tensile strain; this indicates that the spin states of $LaCoO_3$ change drastically according to the magnitude of the tensile strain. On the other hand, in the spectra excited by higher energy (C, D, E, and F), the peaks of d-d excitations are not clear because of the larger fluorescence. Since the d-d excitations were buried in the fluorescence at the excitation energies near L_3 and L_2 edges, we selected the excitation energy

A: $L_3 - 2.9$ eV. Then, we compared the RIXS spectra of the thin films with those of bulk single crystal in order to discuss the relationship between the spin states and the epitaxial strain.

In the analysis, we carried out impurity Anderson model calculations in O_h and D_{2h} local symmetry. Figure 2(a) shows the schematic figures of the crystal structures in bulk and thin film on LSAT(110). The symmetry of bulk is nearly O_h, while that of the thin film on LSAT(110) and LSAT(111) are D_{2h} and D_{3d}, respectively. In the film on LSAT(111), the strain is so small that we consider its symmetry as O_h. Therefore, we performed the calculations in O_h symmetry for the $LaCoO_3$ bulk and the thin film on LSAT(111), while in D_{2h} symmetry for the thin film on LSAT(110). As shown in Fig. 2(b), we consider the $[CoO_6]^{9-}$ cluster model with the scaling factors δ and β in order to describe the crystal distortion, i.e., shrinkage along the [010] axis and elongation along the [001] axis. In the present model, we consider the Co $3d$ orbitals of a central Co atom (core hole site) and appropriate linear combinations of Co $3d$ orbitals on neighboring sites. The

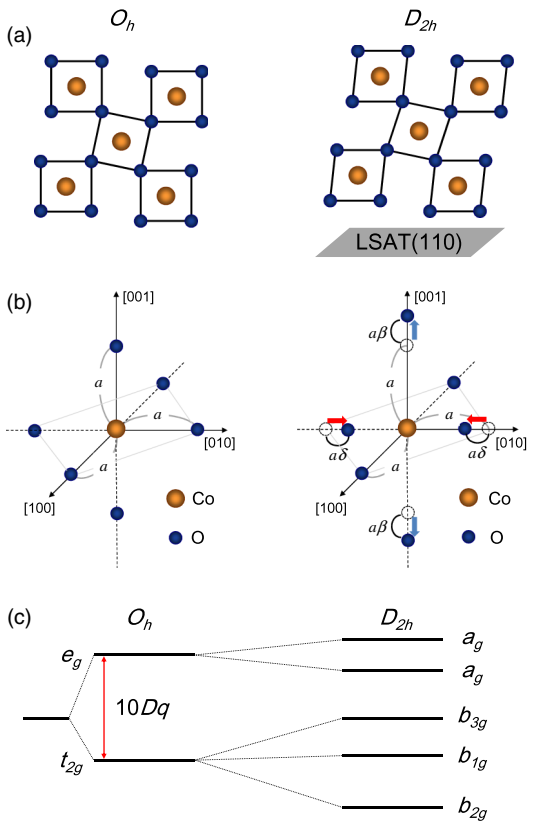

FIG. 2. Schematic view of (a) the crystal structure and (b) $[CoO_6]^{9-}$ cluster in O_h and D_{2h} symmetry. "a" correspond to the bond distance between Co and O ions in $LaCoO_3$ bulk, while "δ" and "β" were defined as the scaling factors of the crystal distortion. (c) The energy level diagram of O_h and D_{2h} symmetry in our calculations. $10Dq$ indicates the crystal field splitting in O_h symmetry.

anisotropic effect due to the lattice mismatch of substrate is also taken into account through the anisotropic hybridization and the crystal field for Co $3d$ states, where the local symmetry around the Co ion is approximately treated as D_{2h}. As shown in Fig. 2(c), the energy diagram in D_{2h} symmetry is different from that in O_h symmetry, where $10Dq$ is defined as the crystal field splitting between the e_g and t_{2g} orbitals. In D_{2h} symmetry, the two energy levels (e_g and t_{2g}) are split into five energy levels by reducing the symmetry, indicating that the new spin states can be realized. In our calculations, the charge-transfer energy from the O $2p$ ligand band to the upper Hubbard band and that from the nonlocal band to the upper Hubbard band are defined as Δ and Δ^*, respectively. In the case of $LaCoO_3$, Ref. [20] shows the importance of the screening effects from neighboring Co ions. The Coulomb interaction between Co $3d$ states (U_{dd}) and that between Co $3d$ and $2p$ core-hole states ($-U_{dc}$) were set as $U_{dd} = 5.6$ and $U_{dc} = 7.0$ eV, respectively. The meaning of these parameters were defined as in Ref. [27]. The Slater integrals and the spin-orbit coupling constant are calculated by Cowan's Hartree-Fock program [28] and then the Slater integrals are rescaled by 85%, as usual. The values of multiplets terms are shown in the Supplemental Material [29]. $(pd\sigma)$ and $(pd\pi)$ are the transfer integrals between Co $3d$ and O $2p$ orbitals and we used the parametrization given in Harrison's rule as $(pd\sigma) \propto d^{-3.5}$ [30]. (d denotes the atomic distance.) In our calculations, the parameters were set as Table II. The spin crossover (HS $\leftrightarrow$ LS) occurs between $10Dq = 1.38$ and 1.40 eV in the O_h symmetry. The value of δ and β in the case of the D_{2h} symmetry were obtained from lattice parameters [11]. Note that the calculations were performed in the wide range of parameters [$10Dq$: 0–4.00 eV, β: 0–0.040, δ: 0–0.040, and $(pd\sigma)$: -3.00–-1.00 eV] and there is no parameter region where the IS state is the most stable.

The experimental RIXS spectra excited with A: $L_3 - 2.9$ eV (776.5 eV) measured at 40 and 300 K are shown in comparison to the theoretical ones with several electronic states in Fig. 3. Although the scattering geometry is different among the samples, the RIXS spectra have no significant polarization dependence as shown in the Supplemental Material [29] and thus we show the calculated spectra for $LaCoO_3$/LSAT(110). There are two kinds of strong peaks in the energy range between 0 and 2 eV in all

TABLE II. Parameter values used in our calculations based on the impurity Anderson model. For details of these parameters, see main text. Units are in eV.

	Δ	Δ^*	$10Dq$	$(pd\sigma)$	δ	β
HS(O_h)	1.1	0.4	1.38	−1.96	0	0
LS(O_h)	1.8	0.7	1.40	−2.00	0	0
HS(D_{2h})	0.2	0.1	1.40	−2.00	0.010	0.005

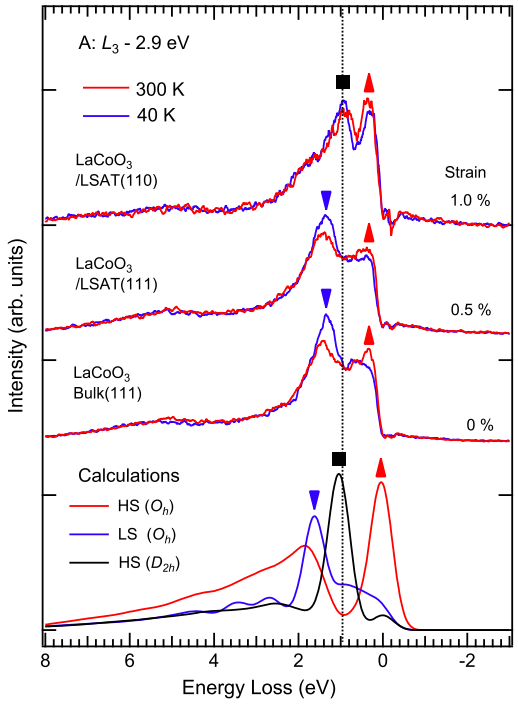

FIG. 3. Temperature dependence (300 and 40 K) of the RIXS spectra excited at A: $L_3 - 2.9$ eV (776.5 eV) in comparison with the impurity Anderson model calculations in O_h and D_{2h} symmetries. These calculations were performed in the scattering geometry for $LaCoO_3$/LSAT(110) and the polarization dependence is shown in the Supplemental Material [29]. The experimental spectra were normalized by their area after subtracting the elastic scatterings by Gaussian fitting. The triangles, squares, and inverted triangles indicate the main peak of the HS(O_h), HS(D_{2h}), and LS(O_h) states, respectively.

three samples. The peaks observed around 0.3 eV can be assigned to the excitations from the HS ground states. On the other hand, the peaks around 1.3 eV observed in $LaCoO_3$/LSAT(111) and bulk correspond to the LS ground states. As the temperature increases, the behavior that the peak intensities at 0.3 eV increase and those at 1.3 eV decrease is consistent with the fact that the population of the HS state increases with increasing temperature. However, peaks which appear at 1.0 eV in $LaCoO_3$/LSAT(110) can be explained by neither the LS nor HS with O_h symmetry. As seen in the theoretical spectra, the peak for the HS state is shifted to 1.0 eV by lowering the symmetry from O_h to D_{2h}. It indicates that the spin state of $LaCoO_3$/LSAT(110) consists of the HS states with different local symmetries, i.e., the mixture of O_h and D_{2h} symmetries. From the temperature dependence, the peak of HS(D_{2h}) still exists at 300 K. It is considered that the spin states are distributed randomly and/or fluctuate quickly after disappearing the spin-orbital ordering at 126 K [11].

To compare the present results with the previous study by resonant x-ray diffraction, we estimate the ratio of spin states by the theoretical spectra of various spin states. Since the theoretical spectra are normalized by the intensity of the

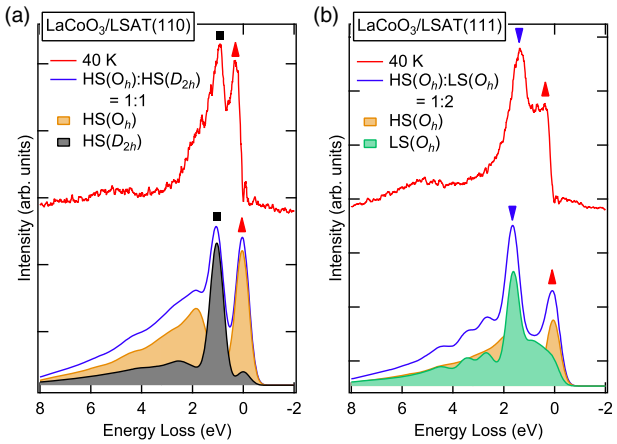

FIG. 4. Comparison between the experimental RIXS and the linear combinations of theoretical spectra in (a) $LaCoO_3$/LSAT(110) and (b) $LaCoO_3$/LSAT(111). The triangles, squares, and inverted triangles indicate the main peak of the HS(O_h), HS(D_{2h}), and LS(O_h) ground states, respectively.

theoretical XAS at A: $L_3 - 2.9$ eV, we can reproduce the mixed spin states by linear combinations of the spectra and estimate the ratio of the spin states by the peak intensity in each spin state. As shown in Fig. 4(a), HS(O_h):HS(D_{2h}) = 1:1 is in good agreement with the experimental spectrum of $LaCoO_3$/LSAT(110), indicating that the CoO_6 octahedra in O_h and D_{2h} local symmetry coexist as the ratio of 1:1. Since the spatial modulation of spin state is fourfold periodic from the x-ray diffraction in Refs. [11,13], one plausible model is that the spin states are aligned in order of O_h-$D_{2h}(d_{yz})$-O_h – $D_{2h}(d_{zx})$, where the HS states with D_{2h} have two different orbital states. In this study, we did not find the theoretical spectra of IS states that reproduce experimental results and thus could not confirm the spin state model of IS:HS = 3:1. On the other hand, HS(O_h):LS(O_h) = 1:2 agrees with the experimental spectrum of $LaCoO_3$/LSAT(111) as shown in Fig. 4(b). The result is consistent with the x-ray diffraction study [12].

In conclusion, the spin states of $LaCoO_3$ change from LS to HS according to the magnitude of the epitaxial strain and the change of the symmetry, which could not be detected by conventional XAS but could be clarified by RIXS measurements. The LS ground state in bulk fully changes to HS states by tensile strain as small as 1.0%. Especially in the thin film on LSAT(110), we observed the tensile-strain induced unique spin state, i.e., HS(O_h):HS(D_{2h}) = 1:1. Since the spin state is not stabilized by temperature or hydrostatic pressure in bulk, applying the tensile strain is an important factor for realizing novel spin states.

The authors thank T. Arima and K. Yamamoto for productive discussions. The present work was performed under the approval of the Synchrotron Radiation Research Organization, the University of Tokyo (Proposals: No. 2016A7501 and No. 2016B7515) and of the Photon Factory Program Advisory Committee, the Institute of

Material Structure Science, High Energy Accelerator Research Organization (Proposal No. 2015S2-007). This work was financially supported by Grants-in-Aid for Scientific Research (Grants No. 16H05990, No. 26105007, and No. 16K17722) from the Japan Society for the Promotion of Science (JSPS). This research was supported in part by PRESTO Grant No. JPMJPR177A from Japan Science and Technology Agency (JST) and by the Murata Science Foundation.

*Present address: National Institute for Materials Science (NIMS), Tsukuba 305-0047, Japan.
YOKOYAMA.Yuichi@nims.go.jp
†Present address: Toshiba Nanoanalysis Corporation Kawasaki, Kanagawa 212-8583, Japan.
munetaka.taguchi@nanoanalysis.co.jp

[1] M. Imada, A. Fujimori, and Y. Tokura, Rev. Mod. Phys. **70**, 1039 (1998).
[2] M. W. Haverkort, Z. Hu, J. C. Cezar, T. Burnus, H. Hartmann, M. Reuther, C. Zobel, T. Lorenz, A. Tanaka, N. B. Brookes, H. H. Hsieh, H.-J. Lin, C. T. Chen, and L. H. Tjeng, Phys. Rev. Lett. **97**, 176405 (2006).
[3] J. Kuneš, J. Phys. Condens. Matter **27**, 333201 (2015).
[4] A. Sotnikov and J. Kuneš, Sci. Rep. **6**, 30510 (2016).
[5] J. Nasu, T. Watanabe, M. Naka, and S. Ishihara, Phys. Rev. B **93**, 205136 (2016).
[6] D. Fuchs, C. Pinta, T. Schwarz, P. Schweiss, P. Nagel, S. Schuppler, R. Schneider, M. Merz, G. Roth, and H. v. Löhneysen, Phys. Rev. B **75**, 144402 (2007).
[7] D. Fuchs, E. Arac, C. Pinta, S. Schuppler, R. Schneider, and H. v. Löhneysen, Phys. Rev. B **77**, 014434 (2008).
[8] J. W. Freeland, J. X. Ma, and J. Shi, Appl. Phys. Lett. **93**, 212501 (2008).
[9] V. V. Mehta, M. Liberati, F. J. Wong, R. V. Chopdekar, E. Arenholz, and Y. Suzuki, J. Appl. Phys. **105**, 07E503 (2009).
[10] A. D. Rata, A. Herklotz, L. Schultz, and K. Dörr, Eur. Phys. J. B **76**, 215 (2010).
[11] J. Fujioka, Y. Yamasaki, H. Nakao, R. Kumai, Y. Murakami, M. Nakamura, M. Kawasaki, and Y. Tokura, Phys. Rev. Lett. **111**, 027206 (2013).
[12] J. Fujioka, Y. Yamasaki, A. Doi, H. Nakao, R. Kumai, Y. Murakami, M. Nakamura, M. Kawasaki, T. Arima, and Y. Tokura, Phys. Rev. B **92**, 195115 (2015).
[13] Y. Yamasaki, J. Fujioka, H. Nakao, J. Okamoto, T. Sudayama, Y. Murakami, M. Nakamura, M. Kawasaki, T. Arima, and Y. Tokura, J. Phys. Soc. Jpn. **85**, 023704 (2016).
[14] M. Abbate, J. C. Fuggle, A. Fujimori, L. H. Tjeng, C. T. Chen, R. Potze, G. A. Sawatzky, H. Eisaki, and S. Uchida, Phys. Rev. B **47**, 16124 (1993).
[15] M. A. Korotin, S. Yu. Ezhov, I. V. Solovyev, and V. I. Anisimov, D. I. Khomskii, and G. A. Sawatzky, Phys. Rev. B **54**, 5309 (1996).
[16] M. Magnuson, S. M. Butorin, C. Såthe, J. Nordgren, and P. Ravindran, Europhys. Lett. **68**, 289 (2004).
[17] A. Podlesnyak, S. Streule, J. Mesot, M. Medarde, E. Pomjakushina, K. Conder, A. Tanaka, M. W. Haverkort, and D. I. Khomskii, Phys. Rev. Lett. **97**, 247208 (2006).
[18] K. Knížek, Z. Jirák, J. Hejtmánek, P. Novák, and W. Ku, Phys. Rev. B **79**, 014430 (2009).
[19] J. Kuneš and V. Křápek, Phys. Rev. Lett. **106**, 256401 (2011).
[20] A. Hariki, A. Yamanaka, and T. Uozumi, J. Phys. Soc. Jpn. **84**, 073706 (2015).
[21] K. Tomiyasu, J. Okamoto, H. Y. Huang, Z. Y. Chen, E. P. Sinaga, W. B. Wu, Y. Y. Chu, A. Singh, R.-P. Wang, F. M. F. de Groot, A. Chainani, S. Ishihara, C. T. Chen, and D. J. Huang, Phys. Rev. Lett. **119**, 196402 (2017).
[22] A. Kotani and S. Shin, Rev. Mod. Phys. **73**, 203 (2001).
[23] S. G. Chiuzbăian, G. Ghiringhelli, C. Dallera, M. Grioni, P. Amann, X. Wang, L. Braicovich, and L. Patthey, Phys. Rev. Lett. **95**, 197402 (2005).
[24] L. J. P. Ament, M. van Veenendaal, T. P. Devereaux, J. P. Hill, and J. van den Brink, Rev. Mod. Phys. **83**, 705 (2011).
[25] Y. Kobayashi, T. Mitsunaga, G. Fujinawa, T. Arii, M. Suetake, K. Asai, and J. Harada, J. Phys. Soc. Jpn. **69**, 3468 (2000).
[26] Y. Harada, M. Kobayashi, H. Niwa, Y. Senba, H. Ohashi, T. Tokushima, Y. Horikawa, S. Shin, and M. Oshima, Rev. Sci. Instrum. **83**, 013116 (2012).
[27] M. Taguchi, A. Chainani, K. Horiba, Y. Takata, M. Yabashi, K. Tamasaku, Y. Nishino, D. Miwa, T. Ishikawa, T. Takeuchi, K. Yamamoto, M. Matsunami, S. Shin, T. Yokoya, E. Ikenaga, K. Kobayashi, T. Mochiku, K. Hirata, J. Hori, K. Ishii, F. Nakamura, and T. Suzuki, Phys. Rev. Lett. **95**, 177002 (2005).
[28] R. D. Cowan, *The Theory of Atomic Structure and Spectra* (University of California Press, Berkeley, CA, 1981).
[29] See Supplemental Material at http://link.aps.org/supplemental/10.1103/PhysRevLett.120.206402 for the details of multiplets terms calculated by Hartree-Fock code and the polarization dependence of the calculated RIXS spectra.
[30] W. A. Harrison, *Electronic Structure and the Properties of Solids* (W. H. Freeman and Co., San Francisco, 1980), Appendix.